We are IntechOpen, the world's leading publisher of Open Access books
Built by scientists, for scientists

6,900
Open access books available

186,000
International authors and editors

200M
Downloads

154
Countries delivered to

Our authors are among the

TOP 1%
most cited scientists

12.2%
Contributors from top 500 universities

CLARIVATE ANALYTICS
BOOK CITATION INDEX
INDEXED

WEB OF SCIENCE™

Selection of our books indexed in the Book Citation Index
in Web of Science™ Core Collection (BKCI)

Interested in publishing with us?
Contact book.department@intechopen.com

Numbers displayed above are based on latest data collected.
For more information visit www.intechopen.com

Thermo-Hydrodynamics of Internally Heated Molten Salts for Innovative Nuclear Reactors

Lelio Luzzi, Manuele Aufiero, Antonio Cammi and Carlo Fiorina
Politecnico di Milano - Department of Energy
Enrico Fermi Centre For Nuclear Studies (CeSNEF)
Italy

1. Introduction

The problem of heat transfer in pipe flow has been extensively investigated in the past. Many different models have been proposed and adopted to predict the velocity profile, the eddy diffusivity, the temperature distributions, the friction factor and the heat transfer coefficient (Kays et al., 2004; Schlichting & Gersten, 2000). However, the majority of such studies give a description of the problem for non-internally heated fluids. Models regarding fluids with internal heat generation have been developed more than 50 years ago (Kinney & Sparrow, 1966; Poppendiek, 1954; Siegel & Sparrow, 1959), giving in most cases a partial treatment of the problem in terms of boundary conditions and heat source distribution, and relying on a turbulent flow treatment that does not seem fully satisfactory in the light of more recent investigations (Churchill, 1997; 2002; Kays, 1994; Zagarola & Smits, 1997). Internally heated fluids are of great interest in the current development of Molten Salt Reactors (MSR) (LeBlanc, 2010), included as one of the six innovative nuclear reactors selected by the Generation IV International Forum (GIF-IV, 2002) for a more sustainable version of nuclear power. MSRs are circulating fuel reactors (Nicolino et al., 2008), which employ a non-classical (fluid-type) fuel constituted by a molten halide (fluoride or chloride) salt mixture playing the distinctive role of both heat source and coolant. By adopting classical correlations for the Nusselt number (e.g., Dittus-Boelter), the heat transfer coefficient of the MSR fuel can be overestimated by a non-negligible amount (Di Marcello et al., 2008). In the case of thermal-neutron-spectrum (graphite-moderated) MSRs (LeBlanc, 2010), this has significant consequences on the core temperature predictions and on the reactor dynamic behaviour (Luzzi et al., 2011). Such influence of the heat source within the fluid cannot be neglected, and thus required proper investigation. The present chapter deals with this critical issue, first summarizing the main modelling efforts carried out by the authors (Di Marcello et al., 2010; Luzzi et al., 2010) to investigate the thermo-hydrodynamics of internally heated fluids, and then focusing on the heat transfer coefficient prediction that is relevant for analysing the molten salt behaviour encountered in MSRs.

The chapter is organized as follows. Section 2 provides a brief description of the Molten Salt Reactors, focusing on their distinctive features, in terms of both sustainability (i.e., reduced radioactive waste generation, effective use of natural resources) and safety, with respect to the traditional configuration of nuclear reactors. Section 3 deals with the study of molten salt heat transfer characteristics, which represent a key issue in the current development of MSRs. In

particular, a "generalized approach" to evaluate the steady-state temperature distribution in a representative power channel of the reactor core is presented. This approach incorporates recent formulations of turbulent flow and convection (Churchill, 1997; 2002), and is built in order to carefully take into account the molten salt mixture specificities, the reactor core power conditions and the heat transfer in the graphite core structure. In Section 4, a preliminary correlation for the Nusselt number prediction is advanced in the case of simultaneous uniform wall heat flux and internal heat generation, on the basis of the results achieved by means of the presented generalized approach. In Section 5, the main conclusions of the present study are summarized.

2. Innovative nuclear reactors based on the molten salt technology

In the recent years, there has been a growing interest in Molten Salt Reactors, which have been considered in the framework of the Generation IV International Forum (GIF-IV, 2002; 2009), because of their several potentialities and favourable features when compared with conventional solid-fuelled reactors (Forsberg et al., 2003; Furukawa et al., 2008; Hargraves & Moir, 2010; LeBlanc, 2010; Renault et al., 2010). Actually, MSRs meet many of the future goals of nuclear energy, in particular for what concerns an improved sustainability, an inherent safety, and unique characteristics in terms of actinide burning and waste reduction (Nuttin et al., 2005), while benefiting from the past experience acquired at ORNL[1] with the molten salt technology.

Different from other GIF-IV projects, a specific reference configuration for the MSR has not been identified yet (GIF-IV, 2009). Current R&D activities on MSRs are devoted to this subject and many reactor configurations have been proposed until now (Luzzi et al., 2011). A molten salt reactor can be designed considering both thermal- and fast-neutron spectrum, and can operate as incinerator or breeder or converter (Forsberg, 2002), in critical or sub-critical (i.e., driven by an external neutron source) conditions. An example of the layout of a typical MSR is given in Fig. 1. The primary molten salt mixture[2] flows through the reactor core (constituted by graphite, if a thermal-neutron-spectrum reactor is under consideration) to a primary heat exchanger, where the heat is transferred to a secondary molten salt coolant. The primary salt then flows back to the reactor core. The heat is generated inside the core directly by the primary molten salt mixture, which plays the distinctive role of both fuel and coolant. The liquid fuel salt typically enters the reactor vessel at 560°C and exits at 700°C, with a pressure of ~1 atmosphere. The secondary coolant loop transfers the heat to the power cycle (a multi-reheat helium Brayton cycle or a steam Rankine cycle) or to an hydrogen production facility (Forsberg et al., 2003).

MSRs are based on a liquid fuel, so that their technology is fundamentally different from the solid fuel technologies currently in use or envisaged in future for the other GIF-IV reactor concepts. Some of the advantages specific to MSRs (for instance, in terms of safety) originate directly from this characteristic, as pointed out in the next subsection. Furthermore, these types of reactor are particularly well adapted to the thorium fuel cycle (^{232}Th-^{233}U), which

---

[1] See www.ornl.gov/info/library or www.energyfromthorium.com/pdf/.

[2] Typically, fluorides of fissile and/or fertile elements such as UF_4, PuF_3 and/or ThF_4 are combined with carrier salts to form fluids. The most common carrier salt proposed are mixtures of enriched (>99.99%) ^{7}LiF and BeF_2 termed "flibe". A critical assessment of the potential molten salt mixtures for MSRs can be found in (Renault et al., 2010).
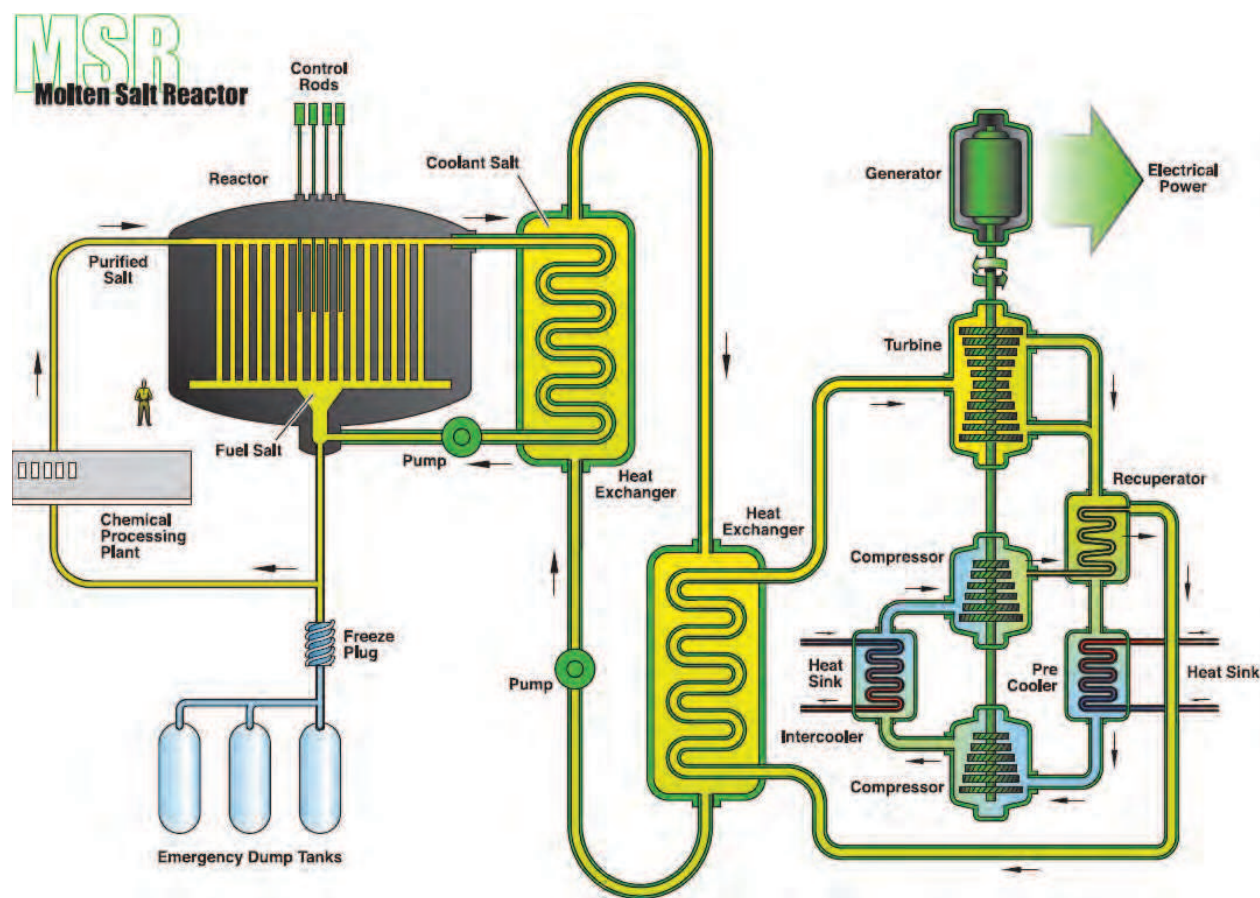
Fig. 1. Schematic representation of a typical MSR (Reproduced from (GIF-IV, 2002))

has the advantage of producing less transuranic isotopes than the uranium-plutonium fuel cycle (^{238}U-^{239}Pu) (Nuttin et al., 2005). Designs specific for the ^{232}Th-^{233}U cycle using fluoride salts have recently been termed Liquid Fluoride Thorium Reactors (LFTR). Among the most attractive features of the LFTR design is the higher sustainability of the back-end of the fuel cycle, in terms of waste profile (Hargraves & Moir, 2010). Adoption of thorium in a closed cycle (i.e., with full recycle of actinides) generates much less waste, of far less radiotoxicity (LeBlanc, 2010), which requires a few hundred years of isolated storage versus the few hundred thousand years necessary for the waste generated by the conventional once-through uranium-plutonium fuel cycle, adopted in the current Light Water Reactors (LWR). LFTRs are featured by a higher fuel cycle sustainability when compared with current LWRs also in terms of natural resource utilization, as can be appreciated looking at the volume of material handled from the front-end phase of the fuel cycle to generate a comparable amount of electric power (Fig. 2).

Besides the favourable features concerning the fuel cycle and the waste management, MSRs offer an array of other advantages in design, operation, safety and proliferation resistance over the traditional solid fuel design of nuclear reactors. A detailed review of such potentialities, as well as of the molten salt technology, is beyond the scope of the present chapter, and can be found in (Furukawa et al., 2008; LeBlanc, 2010; Luzzi et al., 2011; Renault et al., 2010). In the next subsection, the main operational and safety advantages achievable with molten salts
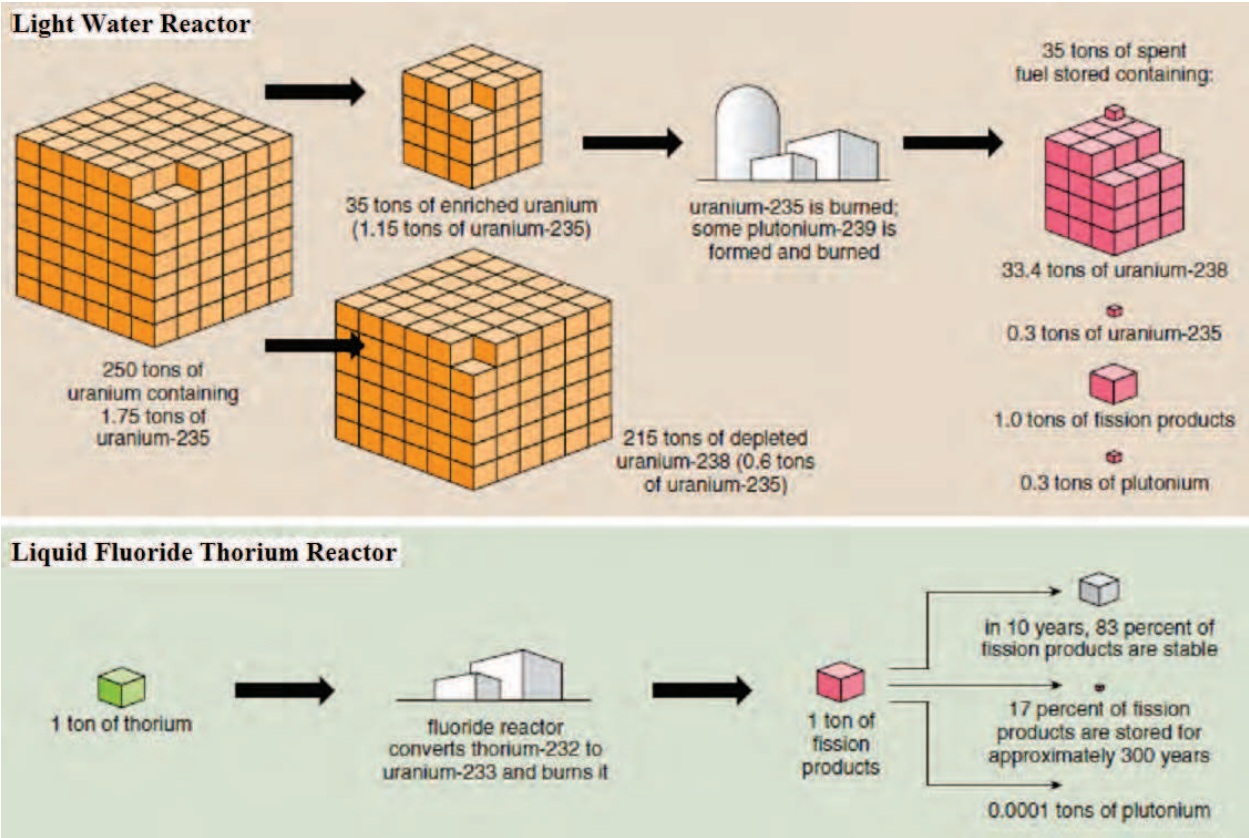
Fig. 2. Mass of material handled from beginning to end to generate comparable amounts of electric power in a LFTR and in a current LWR (Reproduced from (Hargraves & Moir, 2010))

are briefly presented, focusing the attention on the differences with respect to solid-fuelled nuclear reactors.

2.1 Operational and safety issues of MSRs

As the only liquid-fuelled reactor concept, the safety basis and characteristics of the MSR are considerably different from the other reactor concepts. This leads to different advantages, as outlined here below.

The reactor design characteristics minimize the potential for accident initiation. Unlike solid-fuelled reactors, fuel is added as needed, and consequently the reactor has almost no excess nuclear reactivity, which reduces the risk of accidental reactivity insertion. Thanks to a good neutron economy, and to the on-line fuel feeding and reprocessing (in which the fuel is cleaned up from neutron poisons such as Xe), MSRs are usually featured by low fissile inventory. Fission products (except Xe and Kr) are highly soluble in the salt and are expected to remain inside the mixture under both operating and accident conditions. The fission products, which are not soluble (e.g., Xe, Kr), are continuously and relatively easily removed from the molten fuel salt, and the potential for significant radioactivity release from the reactor is notably low.

A distinctive safety feature of the MSR design is that the primary system is at a low operating pressure even at high temperatures, due to the high boiling point ($\sim$1400°C at atmospheric pressure) of the fluoride salt mixture. This eliminates a major driving force (high pressure) for

transport of radionuclides from the reactor to the environment during an accident. Moreover, neutral pressure reduces the cost and the scale of MSR plant construction by lowering the scale of the containment requirements, because it obviates the need to contain pressure like in light water or gas cooled nuclear reactors (featured by thick walled pressure vessels). Disruption in a transport line of the primary system would not result in an explosion, but in a leak of the molten salt, which would be captured in a catch basin, where it would passively cool and harden.

The fluid nature of the fuel means that the reactor core meltdown is an irrelevant term. The liquid state of the core also enables in most emergencies a passive, thermally triggered fuel salt draining into bunkered, and geometrically sub-critical, multiple dump tanks, which are provided with passive decay heat cooling systems (see Fig. 1). Actually, at the bottom of the core, MSR designs have a freeze plug (a plug of salt, actively cooled by a fan to keep it at a temperature below the freezing point of the salt). If the fuel salt overheats and its temperature rises beyond a critical point, the freeze plug melts, and the liquid fuel overflows by gravity and is immediately evacuated from the core, pouring into the emergency dump tanks. This formidable safety tactic is only possible if the fuel is a liquid. Power is not needed to shutdown the reactor, for example by manipulating control elements, but it is needed to prevent the shutdown of the reactor.

Further characteristics of fluoride salts (both fuel and secondary system) are relevant from the safety and design/operational points of view. They are chemically inert, thermodynamically lacking the highly energetic reactions with environmental materials found in other reactor types (e.g., hot zirconium or sodium with water). In particular, the absence of water in the reactor core means no possible steam explosion or hydrogen production within the containment, as occurred in the Fukushima accident. In designs without graphite moderator, there is not even combustible material present. Moreover, molten fluoride salts are excellent coolants, with a 25% higher volumetric heat capacity than pressurized water and nearly 5 times that of liquid sodium. This results in more compact primary circuit components, like pumps and heat exchangers. They also have a much lower thermal conductivity than sodium, thus avoiding thermal shock issues. The high melting temperature ($\sim460°C$ for the "flibe" mixture, $LiF\text{-}BeF_2$ 67-33 mol%) requires operational constraints on reactor temperature to avoid freezing during the normal operating conditions or during maintenance operations, but from the safety point of view it makes molten salt accidentally escaping from the reactor vessel to immediately freeze. Liquid fluoride salts are impervious to radiation damage, which does not constitute a constraint on fuel burn-up limit as for solid-fuelled cores. Actually, they are not subject to the structural stresses of solid fuel and their ionic bonds can tolerate unlimited levels of radiation damage, while eliminating the (rather high) cost of fabricating fuel elements and the (also high) cost of periodic shutdowns to replace them. In addition, a fluid fuel permits to have a homogeneous core composition eliminating the complications connected to the refuelling strategy, which in conventional reactors comprises reshuffling of the fuel assemblies. MSRs can operate with different fissile materials and additives in the liquid fuel, proving the possibility to transmute and burn nuclear wastes such as plutonium, minor actinides and long-lived fission products (Forsberg, 2002).

As concerns inherent safety, MSR designs with fast spectrum (FS-MSRs) are characterized by a very strong negative void (expanded fuel is pushed out of the core) and temperature reactivity coefficients of fuel salt, which avoid the major design constraints required in solid-fuelled

fast reactors and, acting instantly, permit the desirable property of automatic "load following operation". Namely, under conditions of changing electricity demand (load), the reactor tends to adjust its power. Therefore, FS-MSRs can provide a high power density, while maintaining excellent passive safety characteristics (Renault et al., 2010).

In conclusion, the available evidence about the MSR features suggests that the probability and the consequences of a large accident are much smaller than those of most solid-fuelled reactors, whereas the processing system for cleaning the fuel salt and the remote maintenance of major components indicate greater concerns associated with smaller accidents. MSRs involve more intensive manipulation of highly radioactive materials than other reactor classes, and thus small spills and contamination accidents appear to be more likely with this reactor class. The salt processing technology[3] and, more in general, the "liquid salt chemistry" plays a major role in the viability demonstration of MSR concepts and requires essential R&D. Among the main issues, the following ones are worth to be mentioned: (i) the physico-chemical behaviour of coolant and fuel salts, including fission products and tritium; (ii) the compatibility of salts with structural materials for fuel and coolant circuits, as well as fuel processing materials development; (iii) the on-site fuel processing; and (iv) the maintenance, instrumentation and control of liquid salt chemistry (redox, purification, homogeneity). Further details can be found in (Delpech et al., 2010; GIF-IV, 2009). As concerns the modelling efforts, in MSRs a strong coupling between neutronics and thermal-hydraulics exists with more evidence than in solid-fuelled reactors (Cammi et al., 2011a; Křepel et al., 2007; Nicolino et al., 2008). In particular, the following two distinctive features of molten salts (acting both as circulating fuel and coolant) are of relevance for the MSR dynamics and must be properly addressed from the modelling point of view: (i) as it concerns neutronics, the concentration of delayed neutron precursors (DNP) is featured by an unusual pattern according to the fuel velocity field, and can significantly affect the neutron balance since a part of DNPs can decay outside the reactor core (Cammi et al., 2011a; Křepel et al., 2007; Nicolino et al., 2008); (ii) as it concerns thermal-hydraulics, the coolant is a fluid with internal heat generation whose heat transfer properties are considerably different from non-internally heated fluids. To this last issue are dedicated the following sections.

3. A generalized approach to the modelling of the MSR core channels

A typical configuration of a MSR core with a thermal-neutron spectrum is reported in Fig. 3a. It refers to the Molten Salt Breeder Reactor (MSBR) core (Robertson, 1971), usually considered as reference system for benchmark analyses and validation purposes (e.g., Křepel et al. (2007)). The core includes graphite blocks traversed by circular channels (Fig. 3b), through which the power generating molten salt flows. The present work is focused on heat transfer in a single-channel of the core (Fig. 3c), considering the most relevant features related to its physical behaviour modelling, while neglecting the details of the actual geometrical domain. In particular, the analysed geometry consists of a smooth circular channel with constant flow section surrounded by a solid region (represented by the graphite matrix in the specific case of interest), within which the fluid flow is hydro-dynamically developed, but thermally developing, as depicted in Fig. 3d. This situation is consistent with the flow characteristics

---

[3] The molten salt processing technology would include a chemical processing facility for trapping and solidifying the volatile fission products in the off-gas system, and a potential second processing system for removal of the other fission products from the fuel salt.
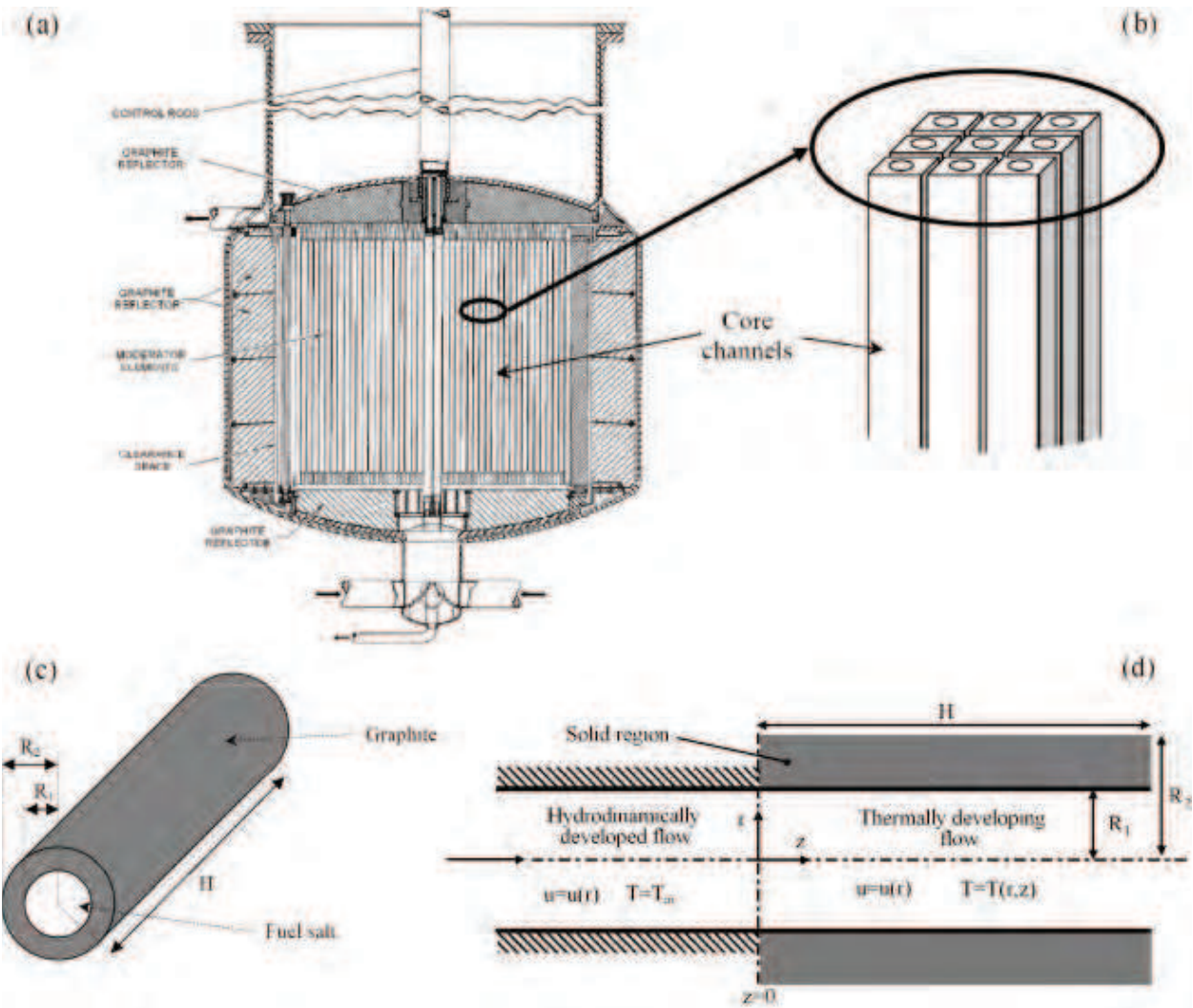
Fig. 3. Schematic representation of the core channel modelling: (a) vertical section of the reactor core; (b) simplified view of the graphite blocks; (c) cylindrical shell approximation of the single-channel; (d) analysed geometry and coordinate system

encountered in the MSR core channels, both in steady-state and transient operation (Luzzi et al., 2011). Even if the graphite blocks can be square or hexagonal shaped, it is a good approximation to model them as a cylindrical shell. In this way, the adopted geometry is axial-symmetric and the use of a two-dimensional domain is made possible.

The analysed physical situation is therefore represented by the molten salt flowing through a cylindrical channel surrounded by graphite, with both the fluid and the solid (see at the end of subsection 3.1) generating power. To properly treat the heat transfer characteristics of such a system, a "generalized approach" is undertaken. This approach treats the problem of heat transfer by forced convection of a fluid inside a circular pipe (generally known as the "Graetz problem") according to a general mathematical formulation that also considers the internal heat generation of the fluid.

In principle, the adopted model is applicable and valid for annular pipes and parallel plate channels but, in the interest of simplicity and practicality, the results are herein limited to circular pipes. The detailed derivation and numerical implementation/discussion of the solution can be found in (Di Marcello et al., 2010; Luzzi et al., 2010), hence in the next two subsections only essential parts are reproduced.

3.1 Mathematical formulation of the generalized approach

With reference to the "Graetz problem", the following expression is adopted for the energy equation:

$$u\frac{\partial T(r,z)}{\partial z} = \frac{1}{r}\frac{\partial}{\partial r}\left[r\left(\frac{\nu}{Pr} + \varepsilon_H\right)\frac{\partial T(r,z)}{\partial r}\right] + \frac{Q(r,z)}{\rho C_p} \tag{1}$$

where the time-averaged axial component of velocity (u) and the eddy diffusivity for heat (ε_H) are assumed to depend only on the radial coordinate (r). For the meaning of the other symbols, see the nomenclature in Section 7. Equation 1 is valid under the following hypotheses: (i) axial-symmetric conditions are taken into account; (ii) steady-state exists; (iii) the fluid is incompressible with no phase change, and constant physical properties; (iv) the hydrodynamic pattern is established; (v) natural convection effects are not considered; and (vi) axial conduction of heat is negligible. The last assumption has been shown by Weigand et al. (2001) to introduce a negligible error for Peclet numbers larger than 10^2. This condition is satisfied in the case of MSRs, which are typically featured by Peclet numbers greater than 10^4. The boundary conditions for Equation 1, at $r = 0$ (at the pipe centreline), must be of the second kind (see Equation 2a) because of assumption (i), while at $r = R_1$ (at the pipe wall) they can be taken as any combination of the boundary conditions of the first, second, and third kind, as expressed by Equations 2b, 2c and 2d, respectively:

$$\left.\frac{\partial T(r,z)}{\partial r}\right|_{r=0} = 0 \tag{2a}$$

$$T(R_1,z) = T_w(z) \tag{2b}$$

$$-k\left.\frac{\partial T(r,z)}{\partial r}\right|_{r=R_1} = j_w(z) \tag{2c}$$

$$T(R_1,z) - \frac{k}{h_w}\left.\frac{\partial T(r,z)}{\partial r}\right|_{r=R_1} = T_E(z) \tag{2d}$$

Finally, the boundary condition at the pipe entrance ($z = 0$) is given by Equation 3:

$$T(r,0) = T_{in}(r) \tag{3}$$

In order to get the solution of the Equation 1 with the boundary conditions 2 and 3, it is convenient to express them in a dimensionless form (see Fig. 4), and then to adopt the so-called "splitting-up procedure". Such procedure consists in splitting-up the solution of the original problem into two parts, as given by Equation 5, and can be applied by assuming that the non-homogeneous term $\Phi(Z)$ and the term $P(R,Z) = R \cdot S(R,Z)$ can be expressed in terms of q-order polynomials of the axial coordinate Z as follows:

Dimensionless form of the energy equation:

$$f(R)\frac{\partial\theta(R,Z)}{\partial Z} = \frac{1}{R}\frac{\partial}{\partial R}\left[R\cdot g(R)\frac{\partial\theta(R,Z)}{\partial R}\right] + S(R,Z) \qquad \text{in } 0 < R < 1$$

Dimensionless form of the boundary conditions:

$$\frac{\partial\theta(R,Z)}{\partial R}\bigg|_{R=0} = 0 \qquad\qquad \theta(R,0) = \theta_{in}(R)$$

$$\alpha\theta(1,Z) - \beta\frac{\partial\theta(R,Z)}{\partial R}\bigg|_{R=1} = \Phi(Z) \begin{cases} \text{(i)} & \alpha=1,\ \beta=0, & \Phi(Z) = \theta_w(Z)\ \text{(first kind)} \\ \text{(ii)} & \alpha=0,\ \beta=1, & \Phi(Z) = J_w(Z)\ \text{(second kind)} \\ \text{(iii)} & \alpha=1,\ \beta=\frac{k}{h_w\cdot R_1}, & \Phi(Z) = \theta_E(Z)\ \text{(third kind)} \end{cases}$$

Dimensionless variables:

$$R = \frac{r}{R_1} \qquad\qquad Z = \frac{2z}{Re\cdot Pr\cdot R_1} \qquad\qquad \theta(R,Z) = \frac{T(r,z)-T^*}{\Delta T}$$

$$\theta_w(Z) = \frac{T_w(z)-T^*}{\Delta T} \qquad \theta_E(Z) = \frac{T_E(z)-T^*}{\Delta T} \qquad \theta_{in}(Z) = \frac{T_{in}(z)-T^*}{\Delta T}$$

$$J_w(Z) = \frac{j_w(z)R_1}{k\cdot\Delta T} \qquad \theta_b(Z) = \frac{T_b(z)-T^*}{\Delta T} \qquad f(R) = \frac{u}{u_{avg}}$$

$$g(R) = \frac{\frac{\nu}{Pr}+\varepsilon_H}{\frac{\nu}{Pr}} \qquad S(R,Z) = \frac{Q(r,z)\cdot R_1^2}{k\cdot\Delta T} \qquad P(R,Z) = R\cdot S(R,Z)$$
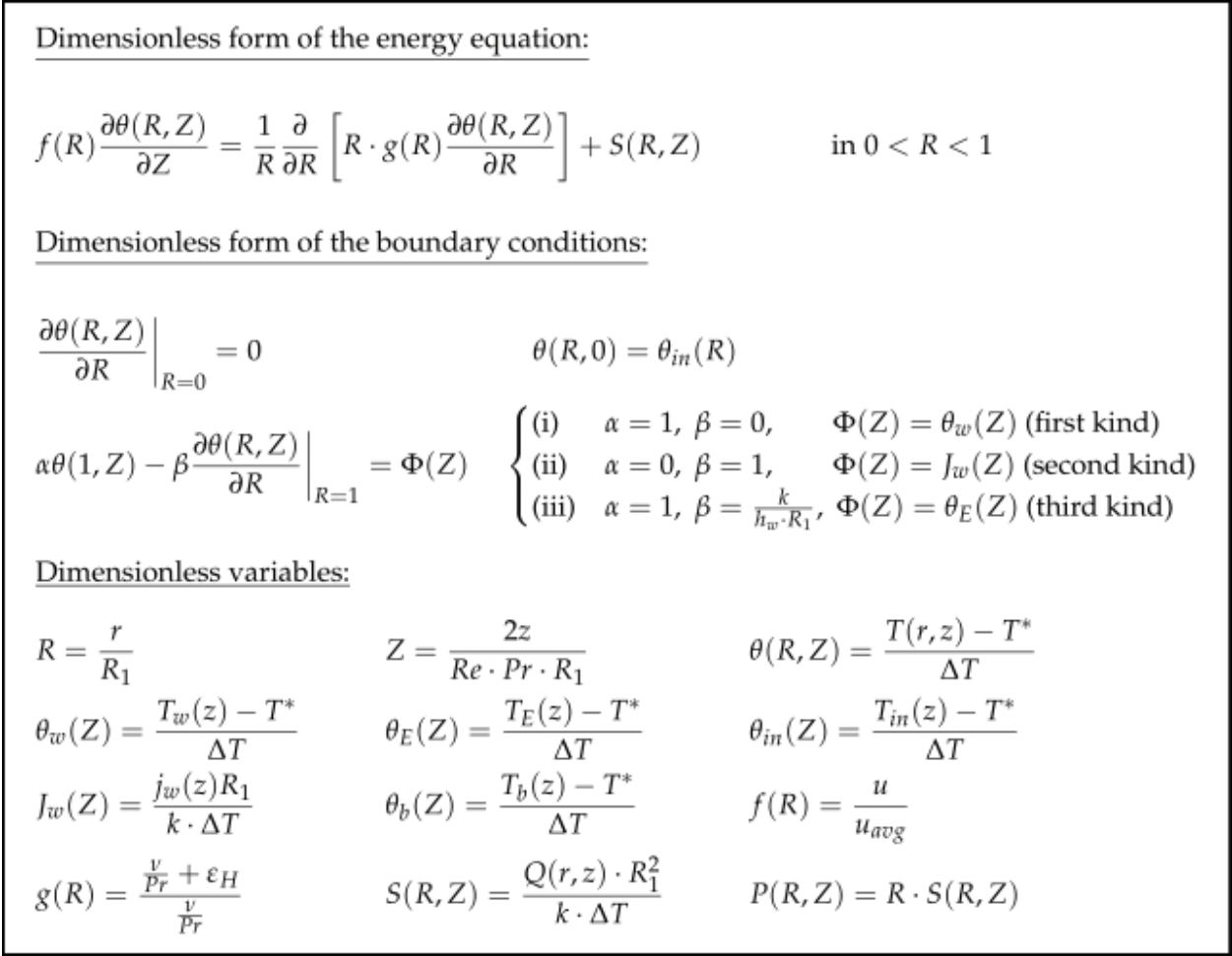
Fig. 4. Dimensionless form of the Equation 1, with the boundary conditions 2 and 3, adopted in the splitting-up procedure

$$\Phi(Z) = \sum_{j=0}^{q}\Phi_j\cdot Z^j,$$

$$P(R,Z) = \sum_{j=0}^{q}P_j(R)\cdot Z^j \tag{4}$$

According to this procedure, the following final solution for the temperature field in the fluid is achieved (details can be found in Di Marcello et al. (2010)):

$$\theta(R,Z) = \sum_{j=0}^{q}\theta_j(R)\cdot Z^j + \sum_{i=1}^{\infty}C_i e^{-\mu_i^2 Z}\Psi_i(R) \tag{5}$$

where

$$C_i = \frac{\int_0^1 R\cdot[\theta_{in}(R)-\theta_0(R)]\cdot f(R)\cdot\Psi_i(R)dR}{\int_0^1 R\cdot f(R)\cdot\Psi_i^2(R)dR} \tag{6}$$

$$\theta_j(R) = \frac{1}{\alpha} \left\{ \Phi_j + \beta \int_0^1 \left[P_j(R) - (j+1)Rf(R)\theta_{j+1}(R) \right] dR \right.$$

$$\left. + \alpha \int_0^1 \frac{1}{Rg(R)} \int_0^R \left[P_j(R') - (j+1)R'f(R')\theta_{j+1}(R') \right] dR'dR \right\}$$

$$- \int_0^R \frac{1}{Rg(R'')} \int_0^{R''} \left[P_j(R') - (j+1)R'f(R')\theta_{j+1}(R') \right] dR'dR'' \tag{7}$$

with $j = q, q-1, q-2, ..., 1, 0$ and $\theta_{q+1}(R) = 0$. In Equation 5, $\Psi_i(R)$ and μ_i are the eigenfunctions and the eigenvalues, respectively, of the Sturm-Liouville problem represented by the differential Equation 8 with its boundary conditions 9:

$$\frac{d}{dR} \left[Rg(R) \frac{d\Psi_i(R)}{dR} \right] + \left[\mu_i^2 Rf(R) \right] \Psi_i(R) = 0 \tag{8}$$

$$\left. \frac{d\Psi_i(R)}{dR} \right|_{R=0} = 0 \tag{9a}$$

$$\alpha\Psi_i(1) - \beta \cdot g(1) \cdot \left. \frac{d\Psi_i(R)}{dR} \right|_{R=1} = 0 \tag{9b}$$

Once the temperature distribution, $\theta(R, Z)$, in the fluid flow is determined, the Nusselt number can be evaluated by means of Equations 10 and 11:

$$Nu(Z) = \frac{2}{\theta(1, Z) - \theta_b(Z)} \cdot \left. \frac{\partial\theta(R, Z)}{\partial R} \right|_{R=1} \tag{10}$$

$$\theta_b(Z) = \frac{\int_0^1 Rf(R)\theta(R, Z)dR}{\int_0^1 Rf(R)dR} \tag{11}$$

In the case of uniform internal heat generation and constant wall heat flux, the dependence of Nu on the axial coordinate vanishes when fully developed flow conditions occur (Di Marcello et al., 2010). This fact will be employed in the derivation of the heat transfer correlation form for internally heated fluids presented in subsection 4.2.

The model described above permits to evaluate in a simple and prompt way some fundamental quantities such as the distributions of temperature and the Nusselt number. It is applicable for: (i) boundary conditions (at the pipe wall) of first, second or third kind, with arbitrary axial distribution; (ii) arbitrary radial distribution of the inlet temperature, $T_{in}(r)$; and (iii) arbitrary shape of the internal heat source $Q(r, z)$ in both the radial and axial directions. The model can be implemented for both laminar and turbulent flow. In the first case, the solution can be obtained by considering the Hagen-Poiseuille parabolic velocity profile and zero eddy diffusivity ε_H, i.e.: $f(R) = 2(1 - R^2)$ and $g(R) = 1$. In the second case, to obtain the velocity profile and the eddy diffusivity for the heat, both needed to solve the original Equation 1, the adoption of a formulation for turbulent flow

is required (see subsection 3.2 for details). In particular, the solution here considered includes the recent formulations of turbulent flow and convection of Churchill (1997) and was assessed for a large variety of fluids, showing that such generalized approach is able to reproduce with a good agreement the experimental data concerning heat transfer evaluations for both fully developed and thermally developing flow conditions, in a wide range of Prandtl ($10^{-2} < Pr < 10^4$) and Reynolds ($2 \cdot 10^3 < Re < 5 \cdot 10^5$) numbers, with and without internal heat generation (Luzzi et al., 2010).

The above generalized approach can be easily extended to evaluate the entire temperature field in the reactor core single-channel, by taking into account the heat conduction in the graphite matrix as well as the corresponding internal heat generation due to gamma heating and neutron irradiation. The "overall solution" (fluid + solid) of such heat transfer problem, with reference to the geometry shown in Fig. 3d, can be achieved by combining the above solution for the turbulent pipe flow of the internally heated molten salt ("Graetz problem") with the solution for the heat conduction problem in the solid region (graphite) surrounding it. The detailed derivation of the "overall solution" can be found in (Luzzi et al., 2010). The final result is shown in Fig. 5, which refers to a single-channel representative of the average steady-state conditions of the MSBR core (Robertson, 1971), shown in Fig. 3a. As far as the boundary conditions are concerned, a constant temperature (T_{in}) is imposed at the channel inlet ($z = 0$), while a convective flux condition is prescribed at the outlet ($z = H$). In the lower part of the solid annulus, at $z = 0$, the same temperature of the fluid entering the channel is fixed. Adiabatic conditions are imposed on the external radius R_2 and in correspondence of the outlet section ($z = H$). On the wall between the fluid and the solid ($r = R_1$), continuity of temperature and wall heat flux are considered.

As can be noticed in Fig. 5, a good agreement is found between the "overall solution" achieved by means of the generalized approach and a dedicated Computational Fluid Dynamics (CFD) simulation. The CFD calculation was performed by means of the finite volume software FLUENT (Fluent, 2005): (i) adopting the incompressible RANS (Reynolds Averaged Navier Stokes) equations for the fluid motion with Boussinesq's eddy viscosity hypothesis; (ii) considering the standard "$k - \varepsilon$ turbulence model" and the enhanced wall treatment approach available in FLUENT; and (iii) in steady-state and hydro-dynamically developed conditions, with reference to a two-dimensional, axial-symmetric (r, z) computational domain, in accordance with the hypotheses and the boundary conditions mentioned above. Further details concerning the mesh strategy and the numerical model are given in (Luzzi et al., 2011).

3.2 Turbulent flow formulation

As pointed out, to obtain the solution of the turbulent "Graetz problem", the reinterpretation of turbulent flow and convection of Churchill (Churchill, 1997; 2002) is considered, so that the eddy diffusivity and thus the velocity profile are expressed in terms of the local turbulent shear stress. In particular, the relationship between the eddy diffusivity for momentum, ε_M, and the dimensionless turbulent shear stress, $(\overline{u'v'})^{++}$, in hydro-dynamically developed flow, is a "one-to-one correspondence" (Churchill, 1997), as expressed in Equation 12:

$$\frac{\varepsilon_M}{\nu} = \frac{\left(\overline{u'v'}\right)^{++}}{1 - \left(\overline{u'v'}\right)^{++}} \qquad (12)$$
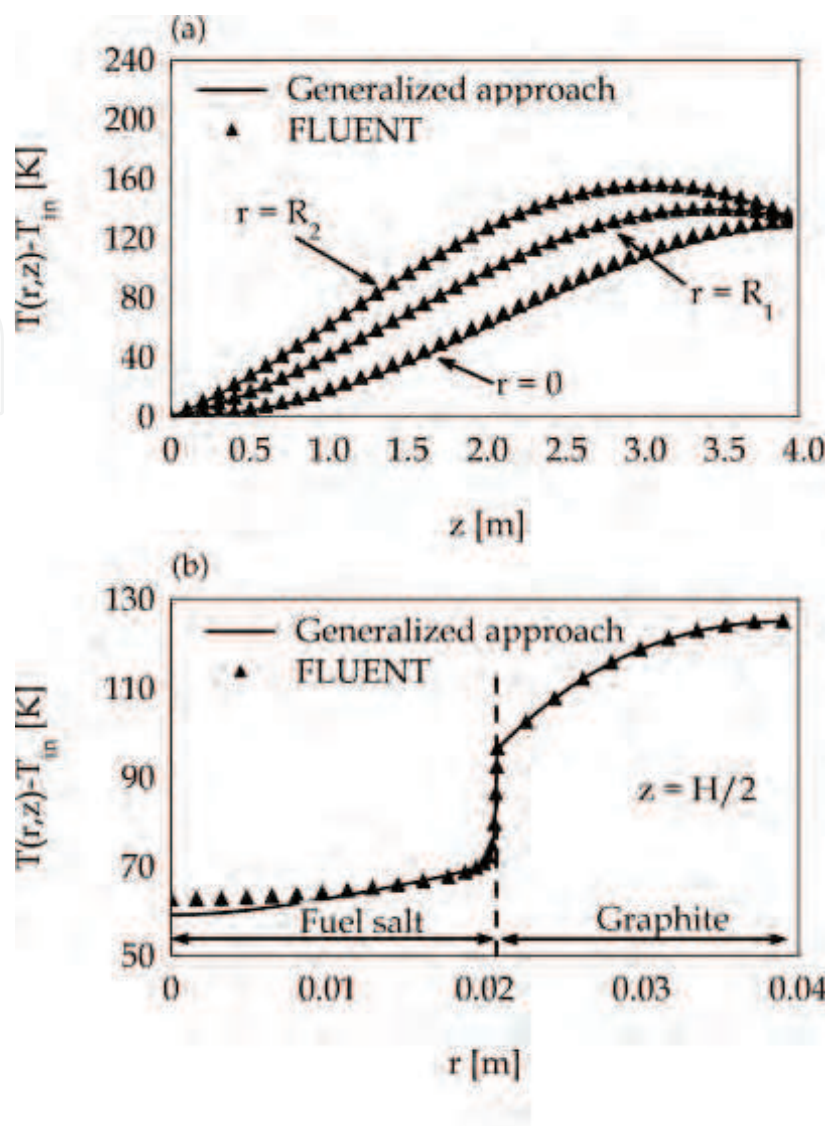
Fig. 5. Axial (a) and radial (b) temperature profile comparison

where

$$\left(\overline{u'v'}\right)^{++} = -\frac{\rho\left(\overline{u'v'}\right)}{\tau} \tag{13}$$

$$\overline{u'v'} = -\varepsilon_M \left(\frac{\partial u}{\partial y}\right) \tag{14}$$

$$\tau = \tau_w \left(1 - \frac{y}{R_1}\right) \tag{15}$$

$$\tau_w = \frac{f}{8}\rho u_{avg}^2 \tag{16}$$

From Equations 12 to 15, the velocity can be obtained as follows

$$u(R) = \frac{\tau_w R_1}{\mu} \int\limits_{R}^{1} R \left[1 - \left(\overline{u'v'}\right)^{++}\right] dR \tag{17}$$

It can be noticed that explicit expressions for the dimensionless turbulent shear stress and the friction factor are required in order to evaluate the velocity profile. For the first one, the following correlation, suggested by Heng et al. (1998) and based on the recent turbulent velocity measurements of Zagarola & Smits (1997), is adopted:

$$\left(\overline{u'v'}\right)^{++} = \left\{ \left| exp\left(\frac{-2.294}{y^+}\right) - \frac{2.294}{a^+}\left(1 + \frac{6.95y^+}{a^+}\right) \right|^{-\frac{8}{7}} + \left[0.7\left(\frac{y^+}{10}\right)^3\right]^{-\frac{8}{7}} \right\}^{-\frac{7}{8}} \quad (18)$$

As far as the Darcy friction factor is concerned, the recent correlation proposed by Guo & Julien (2003) and expressed by Equation 19 is employed, since it predicts the values determined experimentally by Zagarola & Smits (1997) very well, and its form is preferable in terms of explicitness and simplicity:

$$f = \frac{0.3164}{Re^{\frac{1}{4}}}\left(1 + \frac{Re}{4.31 \cdot 10^5}\right)^{\frac{1}{8}} \quad (19)$$

Finally, in order to obtain the eddy diffusivity for heat, ε_H, which is also needed in the solution of the turbulent "Graetz problem" (Equation 1), the turbulent Prandtl number ($Pr_T = \varepsilon_M/\varepsilon_H$) is evaluated through the correlation proposed by Kays (1994), and reported in Equation 20:

$$Pr_T = 0.85 + \frac{0.7}{Pr}\left[\frac{1 - \left(\overline{u'v'}\right)^{++}}{\left(\overline{u'v'}\right)^{++}}\right] \quad (20)$$

This expression was found to be in a good agreement with most experimental and computed values of the turbulent Prandtl number (Kays, 1994).

Fig. 6 shows the comparison in terms of velocity profile between the use of Equation 17 (in the generalized approach) and a CFD calculation performed by means of FLUENT, with reference to the MSBR case (see subsection 3.1). As a result, a general good agreement is found. A more complete study for different Reynolds numbers and different turbulence models is available in (Luzzi et al., 2010). It is worth pointing out that a proper evaluation of the molten salt velocity field is a relevant aspect for what concerns the dynamic behaviour of the MSRs, due to the drift of DNPs and their distribution inside the fluid (Cammi et al., 2011b).

4. Derivation of a heat transfer correlation for the MSR core channels

In the previous section, a detailed treatment of the heat transfer for internally heated fluids has been presented. Treatments of this kind, as well as dedicated CFD codes, can be used to deeply investigate the heat transfer process in many engineering applications. Nevertheless, when dealing with complex systems, computational requirements make often impossible the direct application of such techniques. This is particularly the case for the set-up of models dedicated to the transient analysis of graphite-moderated MSRs, where the reactor core is actually composed by thousands of channels. In this context, it can be useful to rely on a simplified treatment, such as the use of correlations able to predict the Nusselt number, and thus the heat transfer coefficient. In this section, the generalized model presented in subsection 3.1 is adopted to derive a simple correlation for the heat transfer in channels featured by internally heated fluids.
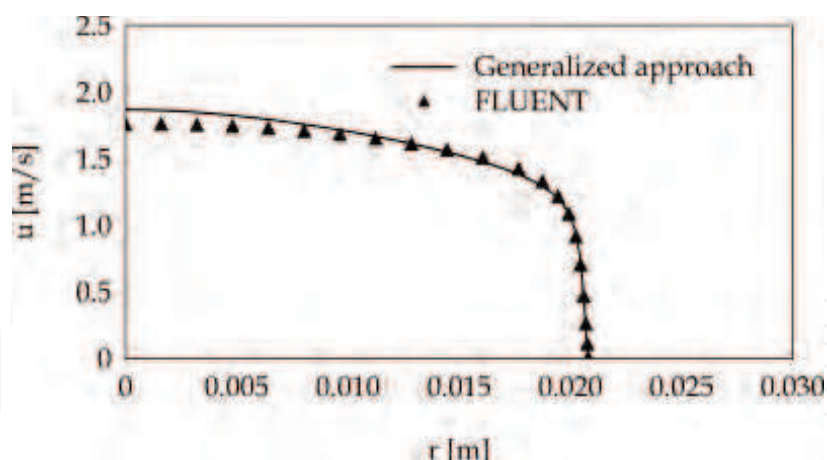
Fig. 6. Velocity profile comparison

4.1 Overview of available correlations

Molten salts are Newtonian fluids and are featured by Prandtl numbers on the order of 10. A number of correlations suitable for a wide range of Reynolds and Prandtl numbers has been proposed in the past, and can be used also for molten salts. Examples of such correlations are the following: the Dittus-Boelter (Dittus & Boelter, 1930), Colburn (Colburn, 1933), and Sieder-Tate (Sieder & Tate, 1936) correlations for turbulent flows; the Hausen (Hausen, 1959) and Gnielinski (Gnielinski, 1976) correlations, which are valid also in the transition between laminar and turbulent flow.

More recent studies have been carried out in order to increase the accuracy of the mentioned correlations for Reynolds and Prandtl numbers of interest in specific fields. As regards molten salts, the Hausen and Gnielinski correlations have been recently checked by means of a dedicated experimental facility, and a slightly modified version of the Gnielinski correlation has been proposed (Yu-ting et al., 2009). Another interesting work can be found in (Bin et al., 2009), where the Sieder-Tate and the Hausen correlations are also assessed, and a modified Sieder-Tate correlation is proposed.

All the correlations mentioned above can be used with a good degree of accuracy in many applications in the field of engineering, but they are not suitable for situations where the working fluid is featured by internal heat generation, as in the case of MSRs. Recently, it has been shown that the use of such classical correlations for predicting heat transfer in MSRs can lead to an underestimate of temperature difference between molten salt and graphite as high as 70% (Luzzi et al., 2010). Specific correlations should then be used for internally heated fluids. Some preliminary studies on the subject are available in literature (Kinney & Sparrow, 1966; Poppendiek, 1954; Siegel & Sparrow, 1959), but they are in most cases partial treatments and they do not lead to the proposal of correlations to be used for turbulent flow.

4.2 Analytical derivation of heat transfer correlation form for internally heated fluids

In this subsection, the problem of heat transfer in channels featured by internally heated fluids is treated analytically, and the general form of the Nusselt number correlation for such situation is derived under the following assumptions: (i) smooth channel with circular cross section; (ii) fully developed turbulent flow conditions; (iii) uniform internal heat generation; and (iv) constant wall heat flux. This situation can be simplified by considering it as the

superimposition of two simpler situations, i.e.: 1) a flow without internal heat generation, but featured by constant wall heat flux, which is the typical case considered by classical heat transfer correlations; and 2) a channel with adiabatic walls and internal heat generation. The possibility of such superimposition is guaranteed by the linearity (with respect to temperature) of the energy equation – see Equation 1. Hence, it is possible to compute the difference between wall and bulk temperatures as follows (see also Fig. 4):

$$(T_w - T_b)_{Q+j_w} = (T_w - T_b)_Q + (T_w - T_b)_{j_w} \tag{21}$$

In Equation 21 and in the next ones, the subscript $Q + j_w$ refers to the complete situation with both internal heat generation and wall heat flux, while the subscripts Q and j_w indicate that the temperature differences are computed in the simplified situation of internal heat generation alone (situation 1) and wall heat flux alone (situation 2), respectively. Introduction of the Equation 21 in the definition of heat transfer coefficient leads to:

$$h_w = h_{Q+j_w} = \frac{j_w}{(T_w - T_b)_Q + (T_w - T_b)_{j_w}} = \frac{1}{\frac{(T_w - T_b)_Q}{j_w} + \frac{(T_w - T_b)_{j_w}}{j_w}} = \frac{1}{h_Q^{-1} + h_{j_w}^{-1}} \tag{22}$$

It should be mentioned at this point that the term h_Q, although similar to h_{j_w} in its definition, does not represent a heat transfer coefficient. Actually, it includes in the same definition the temperatures of the situation 2 (with internal heat generation and with adiabatic walls) and the heat flux in the situation 1 (without internal heat generation). It is possible to rewrite the Equation 22 in terms of Nusselt numbers as follows:

$$Nu = Nu_{Q+j_w} = \frac{1}{Nu_Q^{-1} + Nu_{j_w}^{-1}} = Nu_{j_w} \cdot \frac{1}{1 + \frac{Nu_{j_w}}{Nu_Q}} \tag{23}$$

Equation 23 implies that the Nusselt number, in case of internally heated fluids and constant wall heat flux (Nu_{Q+j_w}), can be computed by means of classical correlations for the value of Nu_{j_w} (subsection 4.1) through the introduction of a correction factor with the form:

$$\gamma = \frac{1}{1 + \frac{Nu_{j_w}}{Nu_Q}} = \frac{1}{1 + \frac{h_{j_w}}{h_Q}} = \frac{1}{1 + \delta} \tag{24}$$

Hence, what is required is the derivation of the term δ as a function of the parameters characterizing the system. Assuming constant the properties of the fluid, it is possible to write:

$$\delta = \delta \left(C_p, \mu, \rho, k, D, u_{avg}, Q, j_w \right) \tag{25}$$

As a matter of fact, some of the dependencies appearing in Equation 25 can be made explicit by means of some physical reasoning, thus reducing the experimental/computational efforts in the derivation of a functional form for δ. By recalling the definition of δ (Equation 24), and introducing the definition of h_Q (Equation 22), it is possible to write:

$$\delta = \frac{h_{j_w}}{h_Q} = \frac{h_{j_w} (T_w - T_b)_Q}{j_w} \tag{26}$$

where h_{j_w} and $(T_w - T_b)_Q$ are independent of j_w. Moreover, the term $(T_w - T_b)_Q$ is directly proportional to Q – see for example (Poppendiek, 1954). It follows:

$$\delta = \frac{h_{j_w} (T_w - T_b)_Q}{j_w} = \frac{Q}{j_w} \varphi \left(C_p, \mu, \rho, k, D, u_{avg} \right) \tag{27}$$

in which the dependence on two parameters has been made explicit. Use of Π-theorem (Langhaar, 1962) in Equation 27 finally leads to:

$$\delta = \frac{QD}{j_w}\varphi(Pr, Re) \tag{28}$$

Summarizing, a correlation for the Nusselt number, in case of simultaneous wall heat flux and internal heat generation, must take the following form:

$$Nu_{Q+j_w} = \gamma Nu_{j_w} = \frac{1}{1+\delta}Nu_{j_w} = \frac{1}{1+\frac{QD}{j_w}\varphi(Pr, Re)}Nu_{j_w} \tag{29}$$

If Nu_{j_w} is assumed to be known from available correlations (subsection 4.1), Equation 29 allows to fully characterize the heat transfer in a channel with internal heat generation simply by finding the dependency of φ upon Reynolds and Prandtl numbers.

4.3 Derivation of a correlation for the Nusselt number in the core channels of MSRs

The results of the previous subsection are of general validity under the mentioned assumptions, and can be used to derive a correlation suitable for computing the Nusselt number in case of channels with internally heated fluids. If the classical correlations available in literature for Nu_{j_w} are adopted, what is required is just the derivation of the function $\varphi(Pr, Re)$. In case of laminar flow ($Nu_{j_w} = 48/11$), the function $\varphi(Pr, Re)$ can be analytically demonstrated to be constant and equal to $3/44$ (Poppendiek, 1954), but, in case of turbulent flow, it can have a complex shape. Nevertheless, by restricting the field of application, it is reasonable to assume a simple dependence such as

$$\varphi(Pr, Re) = a_1 Pr^{a_2} Re^{a_3} \tag{30}$$

where a_1, a_2 and a_3 are constants.

At this point, it is possible to employ the generalized approach described in subsection 3.1 to evaluate the function φ and derive proper values for the constants a_1, a_2 and a_3. In particular, Equation 29 can be rearranged as

$$\varphi(Pr, Re) = \frac{j_w}{QD}\left(\frac{Nu_{j_w}}{Nu_{Q+j_w}} - 1\right) \tag{31}$$

where the Nusselt numbers can directly be computed using Equation 10.

Focusing on the situation encountered in the core channels of graphite-moderated MSRs, Reynolds numbers typically range between 10^3 and 10^5 (Luzzi et al., 2010). Consistently with the choice to use a simple correlation form like Equation 30, the investigation can be restricted to conditions of fully developed turbulence ($Re \geq 10^4$). By employing Equations 31 and 10 as described above, the function φ has been evaluated for 100 different combinations of Prandtl and Reynolds numbers in the ranges $7.5 < Pr < 20$ and $10^4 < Re < 10^5$. Interpolating Equation 30 in the least square sense, the following correlation is finally achieved:

$$\varphi(Pr, Re) = 1.656 \cdot Pr^{-0.4} Re^{-0.5} \tag{32}$$

The average interpolation error results equal to 4.9%, with a maximum error equal to 10.2%. These discrepancies can be considered acceptable for preliminary calculations. It should be

mentioned that, on the basis of the same reasoning here considered, another correlation was presented in (Di Marcello et al., 2010). Such correlation was characterized by a much more complex functional form, but was able to interpolate the data provided by the generalized model with an average error of 3.5%, in the wide range $3 \cdot 10^3 < Re < 2 \cdot 10^5$ and $0.7 < Pr < 10^2$.

Adopting Equation 32, the overall correlation for the Nusselt number, in case of both internal heat generation and wall heat flux, can be written as follows:

$$Nu_{Q+j_w} = \gamma Nu_{j_w} = \frac{1}{1 + \frac{QD}{j_w}\varphi}Nu_{j_w} = \frac{1}{1 + \frac{QD}{j_w}1.656 \cdot Pr^{-0.4}Re^{-0.5}}Nu_{j_w} \quad (33)$$

The MSBR (Fig. 3) can be selected as an example of application. The molten salt that is considered for such reactor is featured by a Prandtl number equal to 11. The Reynolds number in the core channels is on average $2 \cdot 10^4$ (Luzzi et al., 2010). According to these values, the function $\varphi(Pr, Re)$ as computed through Equation 32 results equal to $4.49 \cdot 10^{-3}$. For the MSBR, the ratio QD/j_w is on average equal to 123.4 and, consequently, the correction factor γ results equal to 0.644. This indicates that the direct use of a classical correlation for the Nusselt number would lead to an overestimate of the heat transfer coefficient on the order of 40%. In Fig. 7, the Nusselt number obtained with Equation 33 is compared with some of the correlations available in literature, for Prandtl number equal to 11 and Reynolds numbers lower than 10^5, which is the range of interest for MSRs. For both Equation 33 and Di Marcello et al. (2010), the Gnielinski correlation was used for Nu_{j_w}. The agreement between the two is clearly visible. Overestimate is instead generally observed for the classical correlations, which do not account for the internal heat generation. Such overestimate can be notable at low Reynolds numbers, where Nusselt numbers are over-predicted by as much as four times. In Fig. 7, the results obtained through the use of the CFD code FLUENT (see at the end of Section 3.1 for details) are also shown. They are in a good accordance with the proposed correlation (Equation 33).
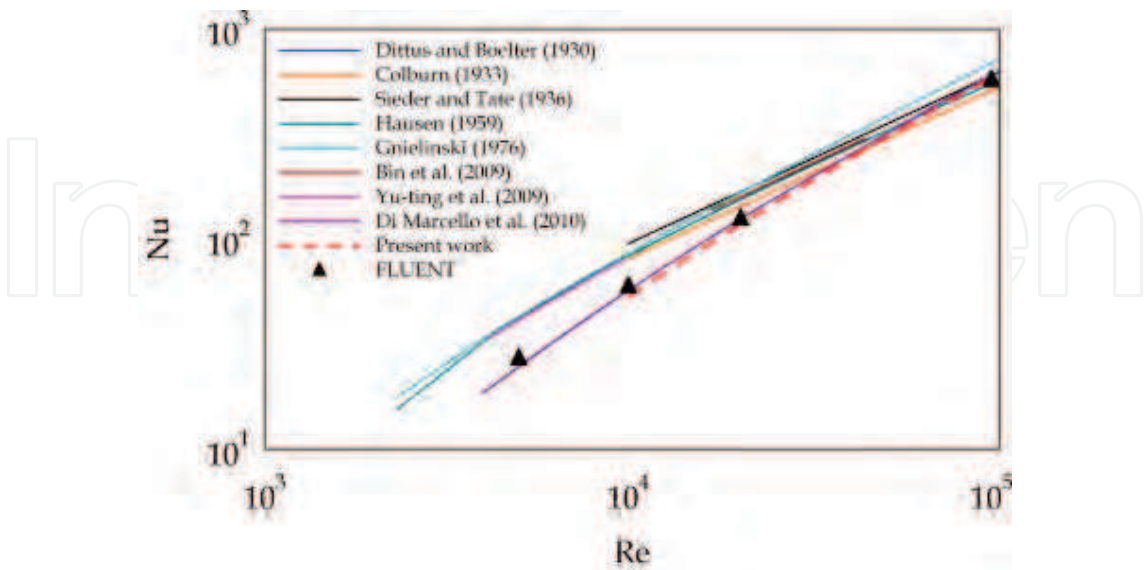

Fig. 7. Comparison among heat transfer correlations, and CFD results, in the Reynolds range of interest for MSRs (Pr=11)

4.4 Possible experimental set-up

The analytical treatment described in the previous sections can provide reasonable results in preliminary studies, but their validity can be tested only through appropriate experimental campaigns. In particular, what is of interest to assess the validity of Equation 33 is the experimental evaluation of the function $\varphi(Pr, Re)$. Equations 26 and 28, together with the definition of Nusselt number, lead to:

$$\varphi(Pr, Re) = Nu_{j_w} \frac{(T_w - T_b)_Q}{\frac{QD^2}{k}} \qquad (34)$$

Assuming Nu_{j_w} as known from available correlations, what is necessary from an experimental point of view is the evaluation of the term $(T_w - T_b)_Q$. This requires a facility able to reproduce the condition of an internally heated, thermally and hydro-dynamically developed turbulent flow in a straight, circular and adiabatic channel (according to the assumptions pointed out at the beginning of subsection 4.2). The experimental set-up must be suitable for measuring wall and bulk temperatures, as well as for ensuring a uniform and precisely-known internal heat generation Q. In addition, the definition of the dependence of φ upon Prandtl and Reynolds numbers requires the capability to vary in a known way the fluid properties, as well as to vary and measure the fluid velocity.

A possible set-up for the thermal-hydraulic circuit required for the experimental analyses of interest was already adopted by Kinney & Sparrow (1966). This set-up was used to test water, but with proper modifications can be adopted also for molten salts. A schematic view of the possible experimental facility is shown in Fig. 8.
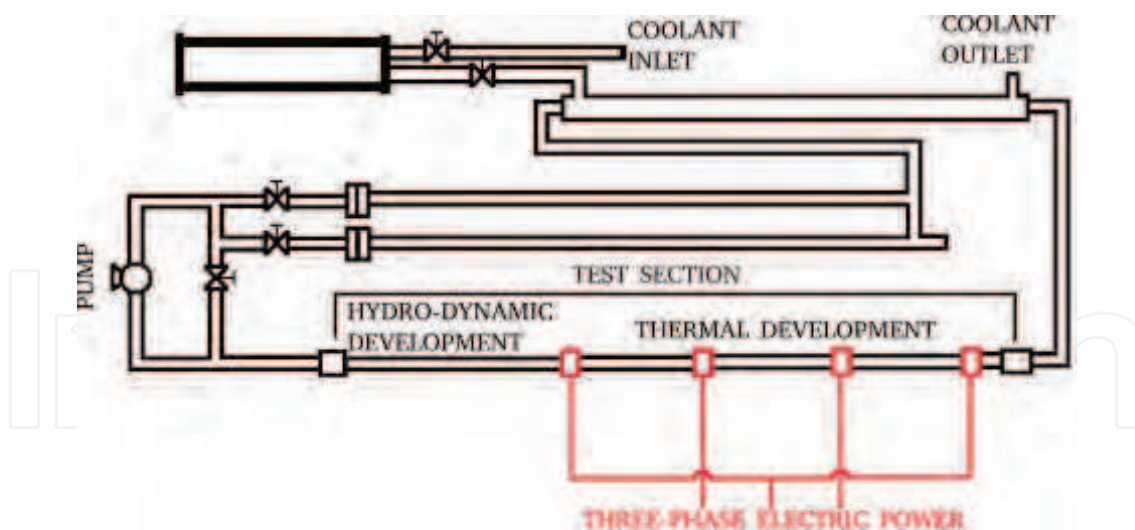

Fig. 8. Schematic view of the possible experimental facility

A closed loop is used, with a heat exchanger for cooling the working fluid, after it has been warmed in the test section. Such test section must be long enough to assure conditions of full thermal and hydro-dynamic development. Internal heating in the fluid is obtained by forcing an electrical current to flow into it. This is possible by choosing an electrically insulating material for the channel wall in the test section, and by placing electrodes at the sides of it.

In this way, the current is forced to flow longitudinally in the fluid. Adopting electricity to heat up the molten salts also solves the problem of the knowledge of the volumetric power Q, which can easily be derived by measuring the electric current in the circuit and the voltage difference at the electrodes. The velocity of the fluid can be varied by using an appropriate pump or valves, and it can be measured by means of standard techniques (e.g., Coriolis flow meter). Wall and bulk temperatures can be measured by means of thermocouples and mixing chambers. Finally, the Prandtl number can be varied by changing fluid, fluid temperature, or by using suitable "thickening" agents (Kedl, 1970).

5. Conclusion

Thermo-hydrodynamics of molten salts is a key issue in the current development of MSRs, which are featured by favourable characteristics with respect to conventional solid-fuelled reactors, due to the peculiarity of a nuclear fuel serving also as coolant, as discussed in Section 2. In this study, a "generalized approach" was undertaken for the "turbulent Graetz problem", with reference to fluids flowing through smooth and straight circular pipes, within which internal heat generation occurs, consistently with the flow characteristics encountered in MSRs. Such generalized model, which incorporates recent formulations of turbulent flow and convection, represents an original contribution in the field of thermo-hydrodynamics, and allows to consider boundary conditions of the first, second and third kind, with arbitrary axial distribution, arbitrary inlet temperature radial distribution and arbitrary variations of internal heat source in both the radial and axial directions. The "overall solution" (molten salt + graphite) presented in Section 3 is thought to be useful under the following two respects: (i) it provides an insight into the heat transfer characteristics of graphite-moderated MSR core channels, as shown for the reference case of the MSBR; (ii) it permits to evaluate in a simple and prompt way some fundamental quantities (i.e., the distributions of temperature and velocity, and the Nusselt number). Moreover, the presented generalized model offers a useful validation framework for assessing CFD codes (Luzzi et al., 2011) and can be an important interpretative support of numerical solutions in steady-state conditions, in the prospect of more complex, multi-physics (thermo-hydrodynamics + neutronics) analyses of graphite-moderated MSR core channels (Cammi et al., 2011a;b). In Section 4, the analytical derivation of the heat transfer correlation form for internally heated fluids was discussed, and a preliminary correlation for the Nusselt number prediction was advanced in the case of simultaneous uniform wall heat flux and internal heat generation, on the basis of the results achieved by means of the "generalized approach". Such correlation, which includes the range of Prandtl and Reynolds numbers of interest for molten salts, provides a simple description of the heat transfer for internally heated fluids, showing that the use of classical correlations (without internal heat generation) for predicting heat transfer in MSRs can lead to an underestimate of graphite temperatures. Although obtained through a detailed analytical treatment, the proposed Nusselt number correlation needs to be verified on experimental grounds. To this purpose, the testing facility and the procedure required for its validation have finally been discussed in brief.

6. Acknowledgment

7. Nomenclature

Latin symbols

a^+	dimensionless pipe/channel radius $\{= R_1 \cdot (\tau_w \cdot \rho)^{1/2}/\mu\}$
a_1, a_2, a_3	coefficients of Equation 30
C_i	coefficients defined by Equation 6
C_p	specific heat, $J \cdot kg^{-1} \cdot K^{-1}$
D	pipe/channel diameter, m $\{= 2R_1\}$
f	Darcy friction factor
$f(R), g(R)$	functions defined in Fig. 4
h, h_w	heat transfer coefficient, $W \cdot m^{-2} \cdot K^{-1}$
H	pipe/channel axial length, m
j	integer number
$j_w(z)$	wall heat flux, $W \cdot m^{-2}$
$J_w(Z)$	dimensionless wall heat flux
k	thermal conductivity of the fluid (molten salt), $W \cdot m^{-1} \cdot K^{-1}$
Nu	Nusselt number
$P(R, Z)$	function defined in Fig. 4 $\{= R \cdot S(R, Z)\}$
$P_j(R)$	j^{th} coefficient of the polynomial expansion of $P(R, Z)$
Pr	molecular Prandtl number
Pr_T	turbulent Prandtl number
q	order of the polynomial expansion of $P(R, Z)$ and $\Phi(Z)$
Q	heat source, $W \cdot m^{-3}$
r	radial coordinate, m
R	dimensionless radial coordinate $\{= r/R_1\}$
R_1	pipe radius/inner radius of the solid (graphite), m
R_2	outer radius of the solid (graphite), m
Re	Reynolds number
$S(R, Z)$	dimensionless internal heat source defined in Fig. 4
t	time, s
T	temperature, K
T^*	reference temperature, K
T_b	bulk (or mixed-mean) temperature, K
$T_E(z)$	external environment temperature, K
$T_{in}(r)$	inlet temperature, K
$T_w(z)$	wall temperature, K
u	axial component of velocity, $m \cdot s^{-1}$
u'	fluctuation in axial component of velocity, $m \cdot s^{-1}$
u_{avg}	average velocity in the pipe/channel section, $m \cdot s^{-1}$
$u_{in}(r)$	axial component of velocity at the pipe/channel inlet, $m \cdot s^{-1}$
$\overline{u'v'}$	time-averaged value of $u'v'$, $m^2 \cdot s^{-2}$
$(\overline{u'v'})^{++}$	dimensionless turbulent shear stress
v'	fluctuation in radial component of velocity, $m \cdot s^{-1}$
y	distance from the wall, m
y^+	dimensionless distance from the wall $\{= y \cdot (\tau_w \cdot \rho)^{1/2}/\mu\}$
z	axial coordinate, m
Z	dimensionless axial coordinate

Greek symbols

α, β	dimensionless coefficients defining the kind of boundary condition at wall
γ	correction factor defined by Equation 24
δ	ratio defined as $(Nu_{j_w}/Nu_Q) = (h_{j_w}/h_Q)$
ΔT	reference temperature difference, K
ε_H	eddy diffusivity for heat, m$^2\cdot$s^{-1}
ε_M	eddy diffusivity for momentum, m$^2\cdot$s^{-1}
$\theta(R, Z)$	dimensionless temperature
$\theta_b(Z)$	dimensionless bulk (or mixed-mean) temperature
$\theta_E(Z)$	dimensionless external environment temperature
$\theta_{in}(R)$	dimensionless inlet temperature
$\theta_j(R)$	functions defined by Equation 7
$\theta_w(Z)$	dimensionless wall temperature
$\theta_0(R)$	dimensionless reference temperature
μ	dynamic viscosity, kg$\cdot$ m$^{-1}\cdot$s$^{-1}\{= \rho \cdot \nu\}$
μ_i	i^{th} eigenvalue of the Sturm-Liouville problem defined by Equation 8
ρ	density, kg$\cdot$m^{-3}
τ	total shear stress, Pa
τ_w	wall shear stress, Pa
ν	kinematic viscosity, m$^2\cdot$s^{-1}
φ	function of Re and Pr, defined as $(j_w \cdot \delta)/(Q \cdot D)$
Φ_j	j^{th} coefficient of the polynomial expansion of $\Phi(Z)$
$\Phi(Z)$	function defining the dimensionless boundary condition at wall
$\Psi_i(R)$	i^{th} eigenfunction of the Sturm-Liouville problem given by Equations 8 and 9

Subscripts

$()_{j_w}$	case of wall heat flux alone (no internal heat generation)
$()_Q$	case of internal heat generation alone (adiabatic wall)
$()_{Q+j_w}$	general case of both wall heat flux and internal heat generation

8. References

Bin, L.; Yu-ting, W.; Chong-fang, M.; Meng, Y. & Hang, G. (2009). Turbulent convective heat transfer with molten salt in a circular pipe. *International Communications in Heat and Mass Transfer*, Vol.36, No.9, pp. 912-916, ISSN 0735-1933

Cammi, A.; Di Marcello, V.; Luzzi, L.; Memoli, V. & Ricotti, M.E. (2011a). A multi-physics modelling approach to the dynamics of Molten Salt Reactors. *Annals of Nuclear Energy*, Vol.38, No.6, pp. 1356-1372, ISSN 0306-4549

Cammi, A.; Fiorina, C.; Guerrieri, C. & Luzzi, L. (2011b). Dimensional effects in the modelling of MSR dynamics: moving on from simplified schemes of analysis to a multi-physics modelling approach. *Nuclear Engineering and Design*, doi:10.1016/j.nucengdes.2011.08.002 (in press), ISSN 0029-5493

Churchill, S.W. (1997). New simplified models and formulations for turbulent flow and convection. *AIChE Journal*, Vol.43, No.5, pp. 1125-1140, ISSN 1547-5905

Churchill, S.W. (2002). A reinterpretation of the turbulent Prandtl number. *Engineering Chemistry Research*, Vol.41, No.25, pp. 6393-6401, ISSN 0888-5885

Colburn, A.P. (1933). A method of correlating forced convection heat transfer data and a comparison with fluid friction. *Transactions of the American Institute of Chemical Engineers*, Vol.29, pp. 174-210, ISSN 0096-7408

Delpech, S.; Cabet, C.; Slim, C. & Picard, G. (2010). Molten fluorides for nuclear applications. *Materials Today*, Vol.13, No12., pp. 34-41, ISSN 1369-7021

Di Marcello, V.; Cammi, A. & Luzzi, L. (2008). Analysis of thermal-hydraulic behaviour of the molten salt nuclear fuel, *Proceedings of the International Conference Nuclear Energy for New Europe*, pp. 301.1-301.10, ISBN 978-961-6207-29-4, Portorož, Slovenia, September 8-11, 2008

Di Marcello, V.; Cammi, A. & Luzzi, L. (2010). A Generalized Approach to Heat Transfer in Pipe Flow with Internal Heat Generation. *Chemical Engineering Science*,Vol.65, No.3, pp. 1301-1310, ISSN 0009-2509

Dittus, F.W. & Boelter, L.M.K. (1930). Heat Transfer in Automobile Radiators of the Tubular Type. *University of California publications in engineering*, Vol.2, No.13, pp. 443-461, ISSN 0096-9311

Fluent, 2005. FLUENT® 6.2 User's Guide, Fluent Inc.

Forsberg, C.W. (2002). Molten salt reactors (MSRs), *Proceedings of the Americas Nuclear Energy Symposium*, Miami, FL, USA, October 16-18, 2002

Forsberg, C.W.; Peterson, P.F. & Pickard, P.S. (2003). Molten-Salt-Cooled Advanced High-Temperature Reactor for Production of Hydrogen and Electricity. *Nuclear Technology*, Vol.144, No.3, (December 2003), pp. 289-302, ISSN 0029-5450

Furukawa, K.; Arakawa, K.; Erbay, L.B.; Ito, Y.; Kato, Y.; Kiyavitskaya, H.; Lecocq, A.; Mitachi, K.; Moir, R.; Numata, H.; Pleasant, J.P.; Sato, Y.; Shimazu, Y.; Simonenco, V.A.; Sood, D.D.; Urban, C. & Yoshioka, R. (2008). A road map for the realization of global-scale thorium breeding fuel cycle by single molten-fluoride flow. *Energy Conversion and Management*, Vol.49, No.7, pp. 1832-1848, ISSN 0196-8904

GIF-IV (2002). A Technology Roadmap for Generation IV Nuclear Energy Systems. Technical Report, GIF-002-00, US DOE Nuclear Energy Research Advisory Committee and the Generation IV International Forum

GIF-IV (2009). Generation IV International Forum 2009 Annual Report, Available from http://www.gen-4.org/PDFs/GIF-2009-Annual-Report.pdf

Gnielinski, V. (1976). New equations for heat and mass transfer in turbulent pipe and channel flow. *International Chemical Engineering*, Vol.16, No.2, pp. 359-367, ISSN 0020-6318

Guo, J. & Julien, P.Y. (2003). Modified log-wake law for turbulent flow in smooth pipes. *Journal of Hydraulic Research*, Vol.16, No.2, pp. 359-367, ISSN 0020-6318

Hargraves, R. & Moir, R. (2010). Liquid Fluoride Thorium Reactors. *American Scientist*, Vol.98, No.4, (July-August 2010), pp. 304-313, ISSN 0003-0996

Hausen, H. (1959). Neue Gleichungen für die Wärmeübertragung bei freier odererzwungener Strömung (new equations for heat transfer in free or forced flow). *Allgemein Wärmetechnik*,Vol.9, No. 4/5, pp. 75-79, ISSN 0002-5976

Heng, L.; Chan, C. & Churchill, S.W. (1998). Essentially exact characteristic of turbulent convection in a round tube. *Chemical Engineering Journal*, Vol.71, No.3, pp. 163-173, ISSN 1385-8947

Kays, W.M. (1994). Turbulent Prandtl number – Where are we?. *Journal of Heat Transfer, Transaction of the ASME*, Vol.116, No.2, pp. 284-295, ISSN 0022-1481

Kays, W.M.; Crawford, M.E. & Weigand, B. (2004). *Convective Heat and Mass Transfer*, McGraw-Hill Inc., ISBN 0070337217, New York.

Kedl, R.J. (1970). Fluid dynamic studies of the Molten-Salt Reactor Experiment (MSRE) core. Technical Report, ORNL-TM-3229, Available from http://www.energyfromthorium.com/pdf/ORNL-TM-3229.pdf

Kinney, R.B. & Sparrow, E.M. (1966). Turbulent pipe flow of an internally heat generating fluid. *Journal of Heat Transfer, Transaction of the ASME*, Vol.88C, No.3, pp. 314-322, ISSN 0022-1481

Křepel, J.; Rohde, U.; Grundmann, U. & Weiss, F.P. (2007). DYN3D-MSR spatial dynamics code for molten salt reactors. *Annals of Nuclear Energy*, Vol.34, No.6, pp. 449-462, ISSN 0306-4549

Langhaar, H.L. (1962). *Dimensional analysis and theory of models*, John Wiley & Sons, ISBN 0882756826, New York.

LeBlanc, D. (2010). Molten salt reactors: a new beginning for an old idea. *Nuclear Engineering and Design*, Vol.240, No.6, pp. 1644-1656, ISSN 0029-5493

Luzzi, L.; Cammi, A.; Di Marcello, V. & Fiorina, C. (2010). An Approach for the Modelling and the Analysis of the MSR Thermo-Hydrodynamic Behaviour. *Chemical Engineering Science*, Vol.65, No.16, pp. 4873-4883, ISSN 0009-2509

Luzzi, L.; Di Marcello, V. & Cammi, A. (2011). *Multi-Physics Approach to the Modelling and Analysis of Molten Salt Reactors*, Nova Science Publishers, Inc., ISBN 978-1-61470-000-5, Hauppauge, NY.

Nicolino, C.; Lapenta, G.; Dulla, S. & Ravetto, P. (2008). Coupled dynamics in the physics of molten salt reactors. *Annals of Nuclear Energy*, Vol.35, No.2, pp. 314-322, ISSN 0306-4549

Nuttin, A.; Heuer, D.; Billebaud, A.; Brissot, R.; Le Brun, C.; Liatard, E.; Loiseaux, J.-M.; Mathieu, L.; Meplan, O.; Merle-Lucotte, E.; Nifenecker, H.; Perdu, F. & David, S. (2005). Potential of thorium molten salt reactors detailed calculations and concept evolution with a view to large scale energy production. *Progress in Nuclear Energy*, Vol.46, No.1, pp. 77-99, ISSN 0149-1970

Poppendiek, H.F. (1954). Forced-convection heat transfer in pipes with volume-heat sources within the fluids. *Chemical Engineering Progress Symposium Series*, Vol.50, No.11, pp. 93-104, ISSN 0069-2948

Renault, C.; Delpech, S.; Merle-Lucotte, E.; Konings, R.; Hron, M. & Ignatiev, V. (2010). The Molten Salt Reactor: R&D Status and Perspectives in Europe, *Proceedings of the 7th European Commission Conference on Euratom research and training in reactor systems*, pp. 384-399, ISBN 13- 978-92-79-13302-2, Prague, Czech Republic, June 22-24, 2009

Robertson, R.C. (1971). Conceptual design study of a single-fluid molten-salt breeder reactor. Technical Report, ORNL-4541, Available from http://www.energyfromthorium.com/pdf/ORNL-4541.pdf

Schlichting, H. & Gersten, K. (2000). *Boundary Layer Theory*, Springer, ISBN 3-540-66270-7, New York.

Sieder, E.N. & Tate, G.E. (1936). Heat transfer and pressure drop of liquids in tubes. *Industrial & Engineering Chemistry*, Vol.28, No.12, pp.1429-1435, ISSN 0888-5885

Siegel, R. & Sparrow, E.M. (1959). Turbulent flow in a circular tube with arbitrary internal heat source and wall heat transfer. *Journal of Heat Transfer, Transaction of the ASME*, Vol.81C, No.1, pp. 280-290, ISSN 0022-1481

Weigand, B.; Kanzamar, M. & Beer, H. (2001). The extended Graetz problem with piecewise constant wall heat flux for pipe and channel flows. *International Journal of Heat and Mass Transfer*, Vol.44, No.20, pp. 3941-3952, ISSN 0017-9310

Yu-ting, W.; Bin, L.; Chong-fang, M.; Meng, Y. & Hang, G. (2009). Convective heat transfer in the laminar-turbulent transition region with molten salt in a circular tube. *Experimental Thermal and Fluid Science*, Vol.33, No.7, pp. 1128-1132, ISSN 0894-1777

Zagarola, M.V. & Smits, A.J. (1997). Scaling of the mean velocity profile for turbulent pipe flow. *Physical Review Letters*, Vol.78, No.2, pp. 239-242, ISSN 0031-9007
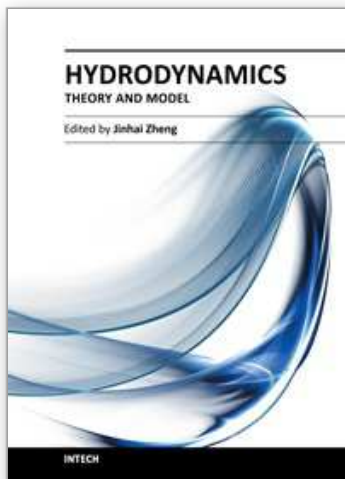
Hydrodynamics - Theory and Model

Edited by Dr. Jin - Hai Zheng

With the amazing advances of scientific research, Hydrodynamics - Theory and Application presents the engineering applications of hydrodynamics from many countries around the world. A wide range of topics are covered in this book, including the theoretical, experimental, and numerical investigations on various subjects related to hydrodynamic problems. The book consists of twelve chapters, each of which is edited separately and deals with a specific topic. The book is intended to be a useful reference to the readers who are working in this field.

How to reference

In order to correctly reference this scholarly work, feel free to copy and paste the following:

Lelio Luzzi, Manuele Aufiero, Antonio Cammi and Carlo Fiorina (2012). Thermo-Hydrodynamics of Internally Heated Molten Salts for Innovative Nuclear Reactors, Hydrodynamics - Theory and Model, Dr. Jin - Hai Zheng (Ed.), ISBN: 978-953-51-0130-7, InTech, Available from: http://www.intechopen.com/books/hydrodynamics-theory-and-model/thermo-hydrodynamics-of-internally-heated-molten-salts-for-innovative-nuclear-reactors

INTECH

open science | open minds